Front. Phys., 2012, 7(6): 679–689
DOI 10.1007/s11467-012-0263-y

REVIEW ARTICLE

Recent progress on the application of LIBS for metallurgical online analysis in China

Feng-Zhong Dong[1,†], **Xing-Long Chen**[2,1], **Qi Wang**[1], **Lan-Xiang Sun**[3], **Hai-Bin Yu**[3], **Yun-Xian Liang**[1], **Jing-Ge Wang**[1], **Zhi-Bo Ni**[1], **Zhen-Hui Du**[4], **Yi-Wen Ma**[4], **Ji-Dong Lu**[5]

[1] *Anhui Institute of Optics and Fine Mechanics, Chinese Academy of Sciences, Science Island, Hefei 230031, China*
[2] *School of Instrument Science & Opto–Electronic Engineering, Hefei University of Technology, Hefei 230009, China*
[3] *Shenyang Institute of Automation, Chinese Academy of Sciences, Shenyang 110016, China*
[4] *College of Precision Instrument & Opto–Electronic Engineering, Tianjin University, Tianjin 300072, China*
[5] *College of Electric Power, South China University of Technology, Guangzhou 510640, China*
E-mail: †*fzdong@aiofm.ac.cn*

Received February 24, 2012; accepted July 4, 2012

Recent progress on the application of laser-induced breakdown spectroscopy (LIBS) for metallurgical analysis particularly achieved by Chinese research community is briefly reviewed in this article. The content is mainly focused on the progress in experimental research and calibration methods toward LIBS applications for metallurgical online analysis over the past few years. Different experiment setups such as single-pulse and double-pulses LIBS schematics are introduced. Various calibration methods for different metallic samples are presented. Quantitative results reported in the literature and obtained in the analysis of various samples with different calibration methods are summarized. At the last section of this article, the difficulties of LIBS application for molten metal analysis in a furnace are discussed.

Keywords laser-induced breakdown spectroscopy (LIBS), metallurgical analysis, molten metal, calibration methods

PACS numbers 52.90.+z

Contents

1 Introduction 679
2 Experimental issues 680
2.1 Laser, spectrograph and detector 680
2.2 Single-pulse and double-pulse LIBS schematics 680
3 Data processing 682
4 Calibration methods 682
4.1 Linear univariate calibration and internal calibration 682
4.2 Calibration-free 683
4.3 Quadratic nonlinear calibration 685
4.4 Artificial neural networks 685
4.5 Quantitative analysis results 686
5 Researches on molten metal on-line analysis 686
6 Conclusions 688
Acknowledgements 689
References 689

1 Introduction

Laser-induced breakdown spectroscopy (LIBS) technique uses a pulse laser to generate plasma which vaporizes a small amount of the sample. Spectra emitted by the excited species, mostly atoms, are used for qualitative and quantitative analysis. LIBS technique has several attributes such as: i) no sample preparation required, ii) quick response, iii) nondestructive examination, vi) capability of remote detection using fiber optics, and v) multiple elements analysis simultaneously. These attributes make LIBS useful in many applications like online analyzing steel and slag composition, in situ detection of soil heavy-metal contamination [1, 2], real-time monitoring material degradation in nuclear reactors [3], environment protection, artwork dating [4–6], and so on.

Analytical control of the continuous casting of molten steel is significant for the quality control of products.

© Higher Education Press and Springer-Verlag Berlin Heidelberg 2012

To realize online analysis of molten steel composition has been considered one of the great difficulties in metallurgical industry. Traditional analytical methods such as X-ray fluorescence (XRF), spark discharge-atomic emission spectroscopy (SD-AES) and inductive coupled plasma–atomic emission spectroscopy (ICP-AES) cannot meet the demands of online measurement, because these techniques need long time in preparing samples. Those unique advantages of LIBS technique mentioned above fit well the application for online composition analysis in metallurgical industry under the harsh environment [7] and have been already demonstrated as the most promising candidate.

Over the past few decades considerable work on LIBS applications for metallurgical industry such as alloy composition analysis and in-process monitoring have been reported. Gruber *et al.* have used LIBS technique for monitoring of Cr, Cu, Mn and Ni in steel by focusing laser beam on the surface of the molten sample in the furnace [8, 9]. Noll *et al.* [10] analyzed the light elements including phosphorus, sulfur and carbon in liquid steel and the estimated limits of detection for these minor elements are lower than 21 μg/g. Noll *et al.* also analyzed slag samples taken from the liquid slag layer in a vacuum degasser station [11] by using a semi-online setup and taking 80 s to fulfill the whole measurement process.

Research on this particular subject in China started relatively late. The first publication focusing on LIBS application in metallurgical analysis in China was made by Yao *et al.* in 2007 [12]. In that paper the authors discussed a LIBS system for fast quantitative analysis of steel near the smelting furnace. They pointed out that the major difficulty for online analysis is from the harsh environment such as high temperature and dusty. Furthermore, they suggested that optic fiber may help to overcome the difficulty. From then on, a few research groups began to involve in this subject. At the present time most of the researches performed have been focusing on the influence of experimental factors, looking for proper spectral calibration methods and carrying on prototype LIBS system developments. Although some meaningful progresses have been gained, the research is still at its early stage of laboratory study.

This paper is intended to briefly review the research progress in the LIBS development specifically for metallurgical analysis achieved by the Chinese scientific community over the past few years. The emphasis is on the experimental results gained and calibration methods toward LIBS applications particularly for metallurgical online analysis.

2 Experimental issues

The performance of LIBS systems mostly depend on both the target sample and experimental condition including the physical / chemical properties of samples, laser parameters, photoelectric detector parameters, measurement parameters, the surrounding environmental parameters, and so on.

2.1 Laser, spectrograph and detector

The basic components of any LIBS system including laser, spectral resolution device and photoelectric detector are similar but the component specifications are tailored to particular applications. For metallurgical analysis, the apparatus used in LIBS are summarized below.

Nd:YAG pulse laser is the major light source used in LIBS measurement. Currently, all research groups dedicated to the LIBS applications on metallurgical analysis choose Nd:YAG pulse laser as the excitation source. The range of laser pulse energy is from 40 mJ to 800 mJ.

The duration of the pulsed laser influence the physical mechanism of plasma generation and evolution. For nanosecond laser pulses, the dominant mechanism is thermal vaporization. For femto-second laser pulses, the primary ablation mechanism is Coulomb explosion. Recently, Fan *et al.* investigated the evolution of electron temperature of Ni plasma with a femto-second pulsed laser [13]. Compared with the plasma induced by nanosecond, the femto-second pulsed laser induced plasma has shorter lifetime and lower electron temperature.

The method of spectral resolution depends on the application and can be as simple as a spectral line filter or a sophisticated Echelle spectrograph. The type of detector depends on many factors such as the spectral range to be monitored and the spectra resolution required. Table 1 lists the spectrometers and detectors used for LIBS in metallurgical analysis.

Temporal resolution is very important for LIBS, especially for calibration free LIBS (CF-LIBS) system. So the intensified CCD (ICCD), which can provide time-gated detection of the laser plasma emission, is a good choice. But ICCD is relatively expensive, other approaches may be used. For instance, Wang *et al.* used a photo-multiplier tube (PMT) and a Boxcar to realize temporal resolution of the emission spectra [14].

Xu *et al.* designed a spectrograph, which placed a CCD on the Rowland circle to detect carbon emission lines [15]. The resolution of the spectrograph reached 0.1 nm.

In addition, experimental parameters have a significant effect to LIBS signal. This has been studied by many research groups [16–18].

2.2 Single-pulse and double-pulse LIBS schematics

Before carrying out studies of online measurement of molten metal, it is necessary to research solid samples,

Table 1 Spectrometer and detector used for LIBS application in metallurgical analysis.

Devices	Characteristics	References
Polychromator and PMT	Wide spectral coverage; temporal response <1 ns;	[12]
Polychromator and CCD	Provide a high resolution over a certain spectral range;	[15]
Grating monochromator, PMT and Boxcar	High sensitivity, time resolution, relatively cheap	[14]
Ocean Optics LIBS2500-7	Wavelength range: 200–980 nm; resolution: 0.1 nm; minimum integral time: 1ms;	[28, 29, 36, 38]
AvaSpec2048FT8RM	Wavelength range: 175–1075 nm; resolution: 0.1 nm; minimum integral time: 2ms;	[33–35, 40]
Echelle spectrograph and ICCD	High resolution: 0.05 nm; broadband spectra coverage: 200-900 nm; time-resolved detection down to few ns;	[18, 22, 24]

such as steel and alloy. For solid samples, the experimental setup is relatively simple. Typically experimental schematic adopted by most research groups is shown in Fig. 1. In this setup, just one pulse laser beam is used to generate plasma. LIBS signal may be weak and unstable in single-pulsed LIBS setup. Wang *et al.* tested double-pulse LIBS system to enhance the signal [19]. Figure 2 shows their experimental setup.

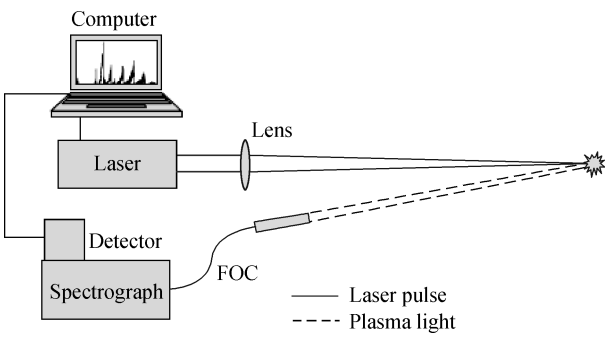

Fig. 1 Typical schematic diagram of single-pulse LIBS apparatus.

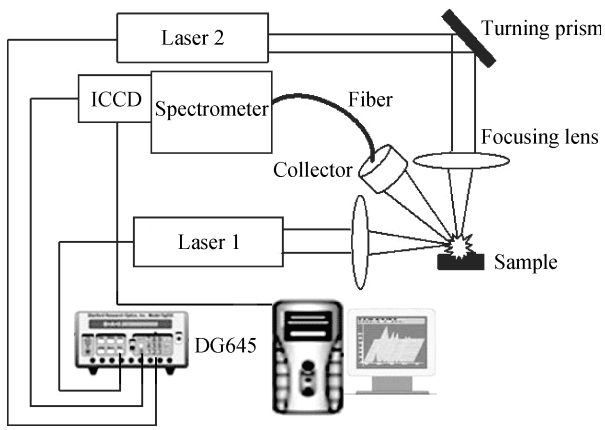

Fig. 2 Schematic diagram of double-pulse LIBS experimental system.

In this double-pulse LIBS system, the directions of two laser pulse beams are orthogonal. The first pulsed laser beam is parallel with the surface of the steel sample. This pulse is focused on the air near the sample surface to ionize air. The second laser pulse, which is used to ablate steel to generate plasma, is vertical with the surface of steel. The intensity of emission from double-pulse LIBS (DP-LIBS) is stronger than that from single-pulse LIBS (SP-LIBS). The spectra recorded in the two schematics are shown in Fig. 3.

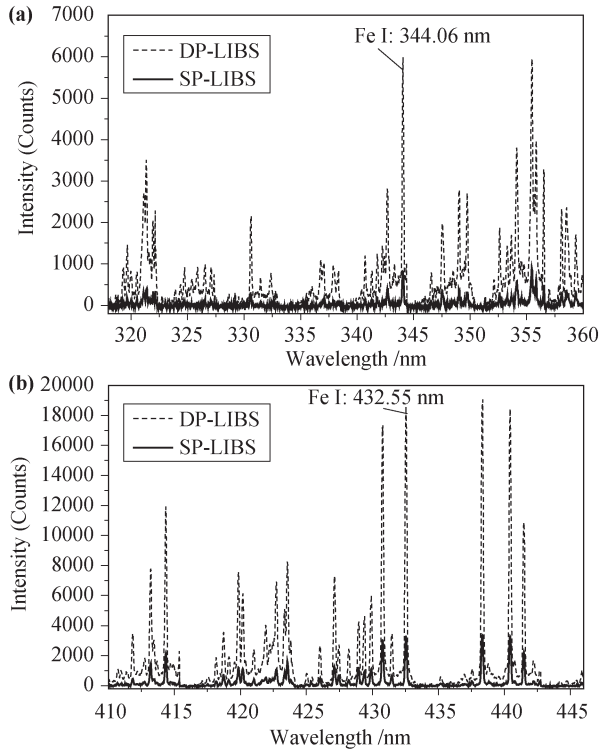

Fig. 3 Emission spectra of steel using single- and double-pulse excitations.

The delay between the two laser beams plays an important role in the enhancement of emission from the plasma. For this purpose, the emission from the plasma was recorded by changing the time delay between the lasers. Figure 4 shows the variation in enhancement of emission intensity from solid steel with increasing time delay between the lasers under double-pulse excitation. Emission intensity was recorded at the gate delay of 0.6 μs, 0.8 μs and 1.0 μs, respectively.

Maximum enhancement in the emission is more than six times at 9 μs for Fe I 497.73 nm. This study shows that it is possible to obtain an optimum enhancement in the line emission for an element by controlling the

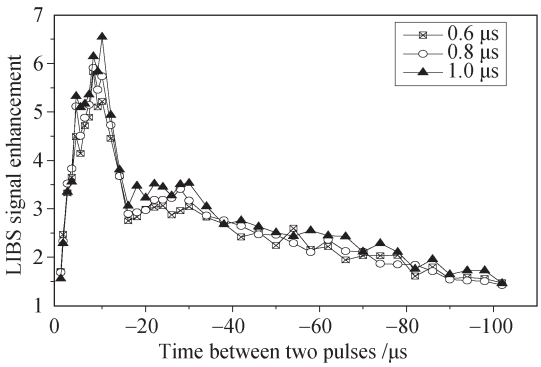

Fig. 4 Ratio of enhancement versus delay time between the lasers.

inter-pulse interval. Some trace elements in steel samples, which cannot be detected in single-pulse excitation, were found in double-pulse excitation. This indicates that double-pulse excitation can improve the sensitivity of LIBS. In fact, the enhancement of line intensity is more obvious for those emission lines when laser pulse energy is high. This is proven in Fig. 5. As a result, more ionic emission lines would be excited and detected.

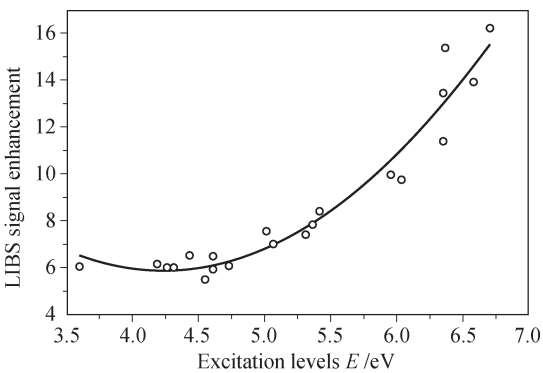

Fig. 5 Variation in signal enhancement with upper level energy.

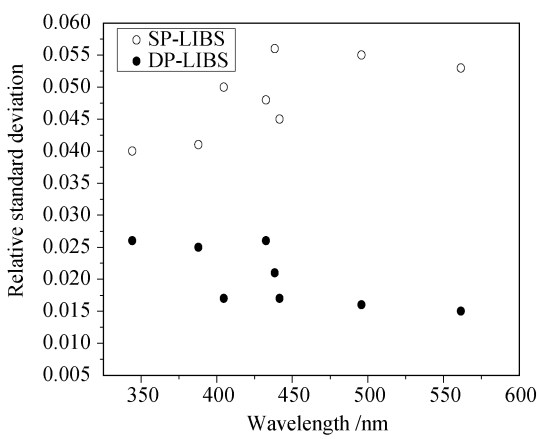

Fig. 6 Comparison of stability of single and double pulse LIBS.

In addition, double-pulse excitation cannot only improve the sensitivity of LIBS, but also improve the stability of emission signal. Wang *et al.* selected eight emission lines of Fe atom as the analytical lines and measure their intensity ten times per line [19]. The relative standard deviation (RSD) of the eight emission line intensities for SP-LIBS and DP-LIBS are shown in Fig. 6, respectively. The smaller RSD indicates that the stability of emission signal in double-pulse excitation is better than that in single-pulse excitation.

3 Data processing

Several groups have applied data analysis techniques to improve the reproducibility of the measurement result. A few of them are reviewed here. Background correction helps to improve the stability of the emission spectra. Because the ambient gas affects the background of the spectrum, this results in poor reproducibility of the spectrum. Sun *et al.* proposed a method that can automatically estimate and correct the varying continuum background emission [20]. In that method all minima on a spectrum were found first, and then the unreasonable minima were deducted by a proper threshold. Finally, one or multiple polynomial functions through the minima left were used to approximate the continuum backgrounds. For slag and steel samples, the estimation of continuum background was shown in Fig. 7.

Spectral data compression helps the data storage and processing. Jiang *et al.* used wavelet transform to compress the spectral data in LIBS [21]. Their result indicated that the amount of storage data was reduced while the main characteristics of the original spectrum were maintained.

4 Calibration methods

4.1 Linear univariate calibration and internal calibration

Ideally, a calibration curve of instrument response versus absolute mass or concentration of the element to be detected is usually linear. This kind of calibration method is relatively simple, therefore it is readily used for quantitative analysis of trace elements in steel.

Wang *et al.* studied the linear calibration curve of Mn in steel samples as shown in Fig. 8 [22]. The determination coefficient R^2 is just 0.709, which is not satisfied. The main reason is that LIBS emission intensity is unstable as a result of matrix effect. In addition, quantitative analysis using this kind of calibration curve is based on the assumption that the excitation conditions for both target samples and the calibrated samples are exactly identical. This is hard to be realized in practice.

To avoid the shortcoming mentioned above, internal calibration is used for quantitative analysis of steel samples. The internal calibration refers the intensities of lines in the target and calibrated samples to some common

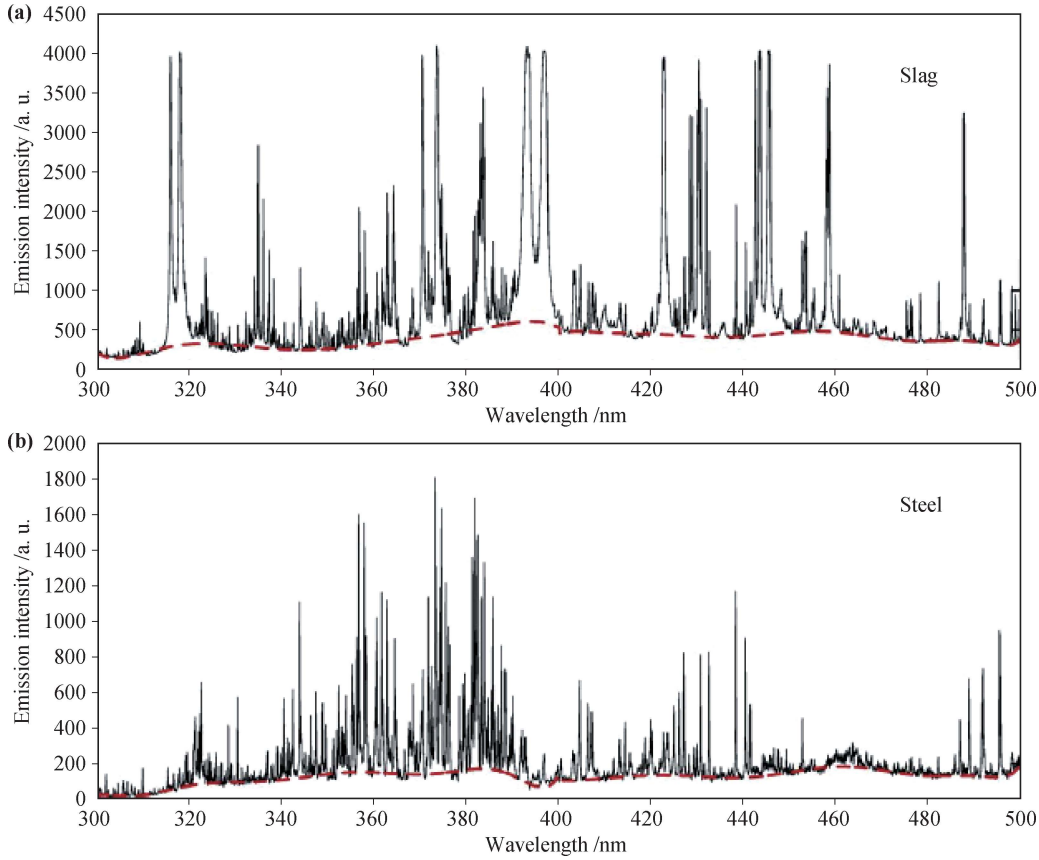

Fig. 7 Estimation of continuum backgrounds for complex LIBS spectra: **(a)** Slag of a converter, and **(b)** low alloy steel.

lines of another element which remains unchanged in both spectra. Such a spectral line is called internal standard because its intensity is also affected by the random fluctuations as that of the element under investigation. The selection of internal reference lines has been discussed in Ref [22]. In Ref [22], the internal calibration curve of Mn, which is shown in Fig. 9, was provided as a comparison of linear calibration curve.

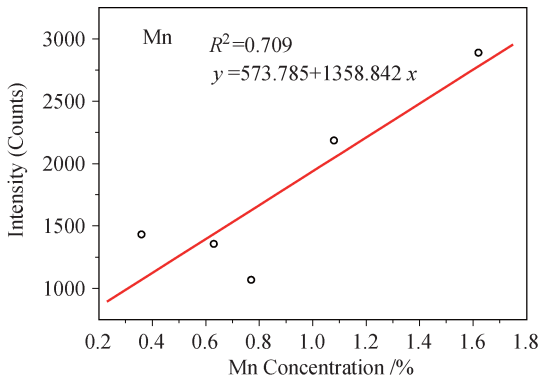

Fig. 8 Calibration curve of Mn I 403.07 nm.

The determination coefficient R^2 of the internal calibration curve is 0.998, which is better than that of a linear calibration curve. This means that the internal calibration can improve the accuracy of the measurement results.

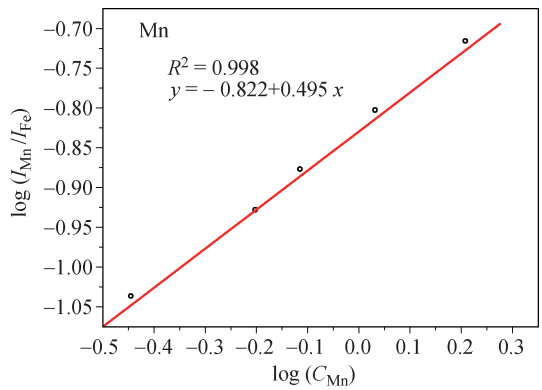

Fig. 9 Internal calibration curve of Mn I 403.07 nm.

It should be pointed out that the mass fraction or concentration of the internal standard element must remain the same in different samples. In steel samples, the mass fraction of Fe is above 95%, so it can be considered an internal standard element. But there is no appropriate internal standard element in slag which also needs to be analyzed in metallurgy industry. So other calibration methods are proposed, such as calibration-free method, artificial neural networks and so on.

4.2 Calibration-free

Calibration-free was first reported by Ciucci *et al.* in

1999. In this method no standard sample is required. Therefore it can reduce the influence of matrix effect on the measuring result. The algorithm used in the CF-LIBS procedure has been described in detail in Ref. [23]. Here we will review only the major points of this approach.

To develop a calibration-free measurement protocol, two reasonable assumptions were adopted: i) the plasma is in local thermodynamic equilibrium (LTE) in the temporal and spatial observation window; ii) the plasma is optically thin for the spectral lines included in the calculation. In LTE, the line integral intensity corresponding to the transition between two energy levels of an atomic species can be expressed as

$$I_{ki} = FCA_{ki}\frac{g_k \mathrm{e}^{-E_k/(k_\mathrm{B}T)}}{U(T)} \tag{1}$$

where $U(T)$ is the partition function of the species at the temperature T, and F is an unknown parameter which accounts for the absolute efficiency of the detection system. F can be determined by normalizing to unit the sum of the species concentration C. A Boltzmann plane can be obtained from a group of spectral lines according to Eq. (1). Finally, the concentration of all the atomic species of the sample can be obtained as

$$C = \frac{U(T)}{F}\mathrm{e}^q \tag{2}$$

where q is the intercept of the fitting curve in Boltzmann plane.

Calibration-free method is used for the quantitative analysis of the slag by Chen *et al.* [24]. To ensure that the plasma is in LTE in the period of measurement, 1 μs delay time and 1 μs integral time is employed. Boltzmann plots for different elements presented in slag were obtained as shown in Fig. 10. The plasma temperature is determined from the Boltzmann plots. In addition, electron density of the plasma is needed, which is determined by Stark broadening of the emission lines.

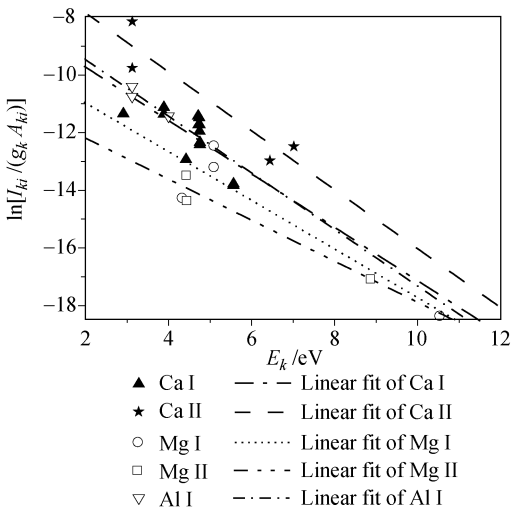

Fig. 10 Boltzmann plots for different elements presented in slag.

The result of quantitative analysis of the slag using CF-LIBS is compared with that using XRF as shown in Fig. 11. The measurement errors are acceptable.

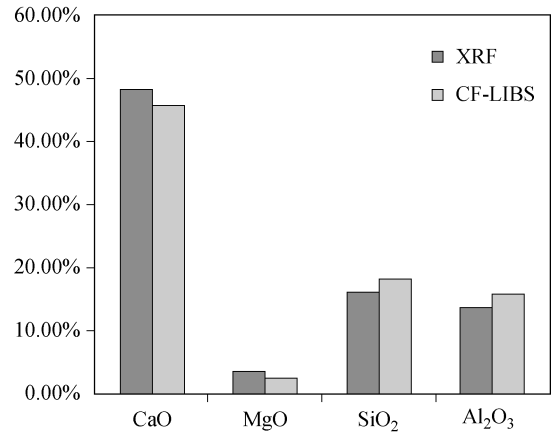

Fig. 11 Comparison of concentrations obtained by CF-LIBS and XRF.

In fact, the above-mentioned assumption is not satisfied in practice. Generally, the plasma generated by laser pulse is in the size of several millimeters, so it is not optically thin. As a result, the intensity of emission lines would be affected by self-absorption. Therefore, self-absorption correction is necessary for an accurate quantitative analysis in CF-LIBS. Bulajic *et al.* used a recursive algorithm based on the curve of growth (COG) to correct the self-absorption effect [25]. This method is complex and hard to implement. A relative simple procedure named internal reference for self-absorption correction (IRSAC) was proposed by Sun *et al.* [26]. In this method, the self-absorption effect of the lines with high excitation energies is considered to be weak. These lines are selected as internal reference lines which are used to approximately measure the self-absorption coefficient of other emission lines.

The Boltzmann plots determined by the basic CF-LIBS method and IRSAC method are shown in Fig. 12 and Fig. 13. As can be seen from the figures, points on the Boltzmann plots linearly stretch and all the fitting

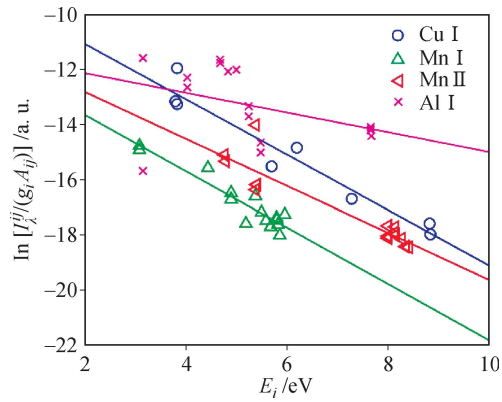

Fig. 12 Boltzmann plots derived from the raw line intensity of the aluminum alloy sample.

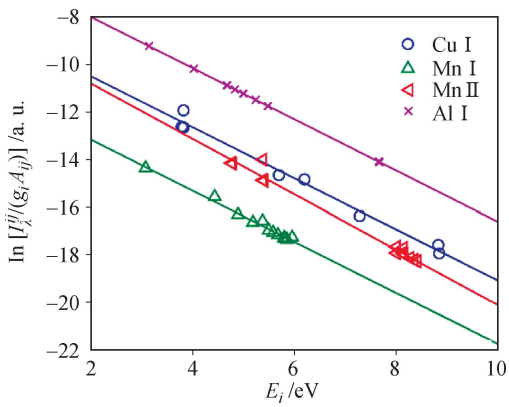

Fig. 13 Boltzmann plots corrected by the IRSAC for the aluminum alloy sample.

lines are almost parallel after correction based on IRSAC method.

The quantitative results determined by the basic CF-LIBS and IRSAC method are given in Table 2 [26]. The IRSAC method can greatly improve the quantitative results based on CF-LIBS.

Table 2 Quantitative results for different samples.

	Element	Concentration/(wt%)			Relative standard deviation/%
		Certified value	Basic CF-LIBS	IRSAC	IRSAC
Aluminum alloy	Cu	3.99	89.54	4.79	20.05
	Mn	0.81	0.45	0.47	41.98
	Al	83.89	4.40	83.46	0.51
	Other elements	11.31	–	–	
Iron–chromium alloy	Cr	14.26	28.07	13.32	6.59
	Fe	84.54	71.93	86.68	2.53
	Other elements	1.2	–	–	
Iron–chromium–nickel alloy	Cr	28.24	68.92	29.90	5.88
	Fe	40.57	21.25	41.61	2.56
	Ni	24.28	2.91	21.59	11.08
	Other elements	6.91	–	–	

In smelting process, CF-LIBS can only provide a semi-quantitative estimation of the trace components, because even a small uncertainty affecting the result for the major components will lead to a huge relative error affecting the minor components.

4.3 Quadratic nonlinear calibration

A calibration model using a second-order polynomial nonlinear multivariate inverse regression was established to reduce the influence of matrix effect by Laville *et al.* [27]. Here the approach is simply reviewed. For a given component labeled by j (where $1 \leqslant j \leqslant m$), the linear multivariate inverse regression method limited to the second-order consists in writing:

$$[C_j] = [U][B_j] + [e_j] \tag{3}$$

where

$$\boldsymbol{B} = \begin{pmatrix} b_{0,j} \\ b_{1,j} \\ \cdots \\ b_{2n,j} \end{pmatrix} \tag{4}$$

$$\boldsymbol{U} = \begin{pmatrix} 1 & I_{1,1} & \cdots & I_{1,m} & (I_{1,1})^2 & \cdots & (I_{1,m})^2 \\ 1 & I_{2,1} & \cdots & I_{2,m} & (I_{2,1})^2 & \cdots & (I_{2,m})^2 \\ \cdots & \cdots & \cdots & \cdots & \cdots & \cdots & \cdots \\ 1 & I_{n,1} & \cdots & I_{n,m} & (I_{n,1})^2 & \cdots & (I_{n,m})^2 \end{pmatrix} \tag{5}$$

n is the number of samples used to establish the calibration and m the number of components of interest (m is also the number of emission lines). B is a vector containing the unknown parameters of the regression model. $[e_j]$ is the vector of the residuals which corresponds basically to the discrepancies between the prediction given by the multivariate regression model and linear regression obtained with the multivariate results.

Sun *et al.* used this approach to calibrate Mn and Cr in steel samples, and obtained a better result comparied with univariate linear calibration method [28]. They selected 15 steel samples as calibration set, and 5 steel samples as test set. The RSD and relative mean square error (RMSE) of the quantitative results using linear univariate calibration and quadratic nonlinear calibration are determined, respectively. The smaller RSD and RMSE reveal a better reproducibility and precision. Table 3 indicates that quadratic nonlinear calibration can take a full advantage of spectra information to obtain a better measurement result.

Table 3 Results quantified for LIBS for multi-matrix steel samples.

Method	Element	Concentration	R^2	RSD	RMSE
Linear univariate calibration	Mn	0.058–2.53	0.693	21.29	0.465
	Si	0.031–1.99	0.904	22.95	0.167
Quadratic nonlinear calibration	Mn	0.058–2.53	0.990	7.38	0.073
	Si	0.031–1.99	0.998	9.51	0.023

4.4 Artificial neural networks

Artificial neural network (ANN) algorithms are now being used in a wide variety of data processing applications. There are many kinds of ANN. Back propagation (BP) networks in LIBS application is commonly used for nonlinear prediction. Sun *et al.* used BP network to predict the contents of Mn and Si in steel samples, and stud-

ied the influence of various inputs on the outputs of the ANN [29]. They compared the performance of the neural networks with peak intensity inputs and integral intensity inputs. Their results show that the suitable inputs can result in a satisfying prediction. Liang *et al.* also applied BP network to quantitatively analyze the contents of MgO and CaO in slag samples [30]. They found that using the integral intensity of the line as the input of the ANN cannot take a full advantage of the spectral information. Adding a specified region of background spectrum to the input could obtain a better prediction result.

The structure and inputs of the neural network is crucial to the success of the application. The essence of components prediction using BP network in LIBS is to seek the relation between element component and spectral information. Usually, the relation is complex because of random disturbance and this greatly limits the accuracy of the prediction using ANN.

4.5 Quantitative analysis results

The purpose of developing various calibration methods is to realize quantitative analysis. Many parameters affect the precision and accuracy of a measurement. A list of LIBS measurements for metallurgical analysis is summarized in Table 4.

The RSD, limit of detection (LOD) and relative error represent the repeatability, sensitivity and accuracy of the measurements. Table 4 indicates that LIBS measurement results are related to the element type as well as the calibration methods. Compared to metallic elements, nonmetallic elements are hard to be excited and detected as their most strong lines are in the range of vacuum ultraviolet.

5 Researches on molten metal online analysis

The final goal of metallurgical analysis is the online measurement of the molten metal. The plasma property of molten metal is different from that of solid metal. There are more difficulties for the analysis of molten metal: i) the intensity of background emission is very strong because of the high temperature of the melt. This may result in the emission line of trace element submerged by the background emission; ii) the change in temperature of molten metal influences the emission spectra of the plasma; iii) the chemical reaction in molten metal is very complex; iv) the design of the fire-resistant optical probe is a challenge.

Table 4 Measurement results of LIBS for metallurgical analysis.

Sample	Elements	Calibration method	Results	Reference
Solid steel (GBW01605-01609, GBW01211-01216, GSB03-2028-1-2006	Mn, Si	Multivariate quadratic non-linear function	RSD<10%	[28]
		Artificial neural networks	RSD<8%	[29]
Liquid steel Q235	Cr, Ni, Si, Mn	Internal calibration	Cr: LOD=256ppm, RSD<5% Ni: LOD=166ppm, RSD<8% Si: LOD=109ppm, RSD<8% Mn: LOD=246ppm, RSD<6%	[37]
Solid aluminum alloy	Si, Fe, Cu, Mn, Mg, Zn, Sn, Ni	Internal calibration	LOD:70-1800ppm RSD:2%-4%	[39]
Ferrochrome GBW01424, GBW01425A	Si	Internal calibration	Relative error<4%	[31]
Solid stainless steel GSBH40045-93	Cr, Mn, Al, Cu	Multi-lines Intensity normalization	Cr: RSD<2% Mn,Cu: RSD<4% Al: RSD<8%	[40]
Liquid steel	Mn, Si, Cr	Intensity-concentration linear calibration	Mn: RSD<5%, LOD=76ppm Si: RSD<8%, LOD=24ppm Cr: RSD<5%, LOD=725ppm	[33]
Solid aluminum alloy	Fe, Si, Cu	Intensity-concentration linear calibration	Fe: LOD=104ppm Si: LOD=63ppm Cu: LOD=113ppm	[18]
Solid steel	Mn, Cr	Internal calibration	Mn: LOD=50ppm Cr: LOD=406ppm	[22]
Solid steel	Mo	Intensity-concentration linear calibration	Relative error < 8%	[14]
Solid aluminum alloy GBW02221	Al, Cu, Mg, Mn, Fe, Si, Zn	Calibration free	Relative error < 20%	[41]
Solid slag	CaO, SiO_2, Al_2O_3, MgO	Calibration free	Relative error: CaO<5% SiO_2,Al_2O_3 <15% MgO<30%	[24]

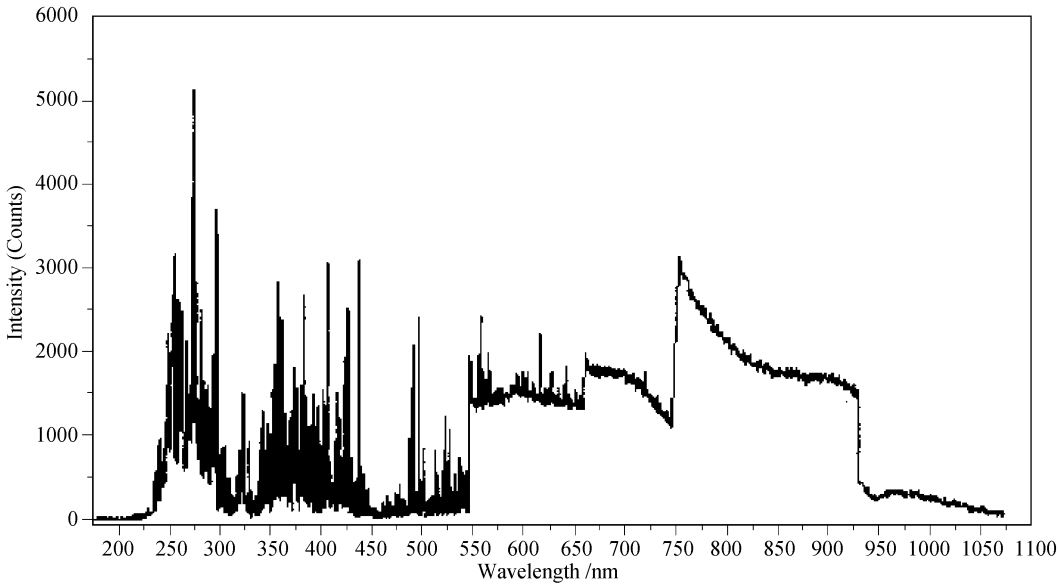

Fig. 14 The emission spectrum of liquid steel in the range of 175–1050 nm.

To solve the above problems, some related researches have been carried out. Lin *et al.* developed an experimental system to semi-online measure Si component in AOD furnace [31]. Because a thick layer of slag floating over the molten metal fluctuates strongly, it is very difficult to analyze the molten metal in furnace directly. So they developed a sample cell near the outlet of the furnace and a sublance sampler which is used to convey fusant from furnace to sample cell. To protect the optic fiber probe from high temperature, the probe is covered by a ceramic pipe.

One effect of the high temperature of molten steel is oxidation of the liquid steel surface. In fact, there is a thick layer of slag on the surface of the molten steel in smelting process. However, in laboratory, molten steel were obtained by melting solid steel in an intermediate-frequency-induction-furnace. So the surface of molten steel may be oxidized in air, and the oxide layer will affect the LIBS signal [32]. Chen *et al.* compared the plasma spectra of molten steel in air and in argon [33]. The result demonstrated that the argon atmosphere cannot only prevent oxidation of the molten steel but also increase the emission intensity of the plasma.

The other effect of the high temperature of the melt is to cause a strong background emission, especially in the band of lower frequency. Figure 14 is the emission spectrum of liquid steel, which shows a strong emission above 550 nm [34].

The high temperature of liquid steel has many other far-reaching influences. Dong *et al.* compared the plasma temperature and plasma electron densities of molten steel and solid steel, respectively [35]. They found that both plasma temperature and plasma electron density of molten steel was higher than that of solid steel, as shown in Fig. 15. The reason is that the atoms and electrons are more active in molten steel because of its high temperature, so the plasma can be formed easily and absorb more laser energy.

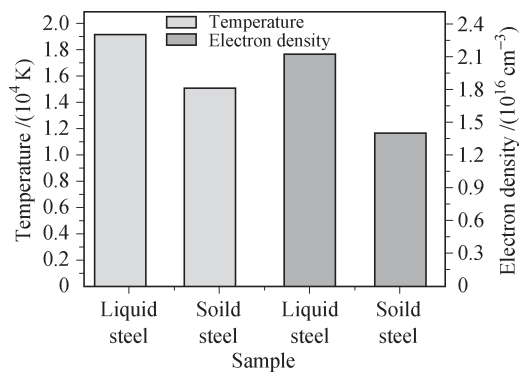

Fig. 15 Comparison of plasma characteristics of liquid steel and solid steel.

Sun *et al.* found that the emission intensities of Cr, Mn, Si decreased exponentially with the decrease of the liquid steel temperature, but the emission intensities of Fe lines did not change significantly with different liquid steel temperatures [36]. Therefore, the internal calibration is useless to reduce the effect of the temperature fluctuation. In this case, it is very important to keep liquid steel temperature constant.

A key factor of quantitative analysis of molten steel is the choice of the analytical lines. This is pointed out in Refs. [18, 29, 31, 33]. The emission lines of Fe are plentiful in molten steel, which can result in spectral line interference. There is no uniform criterion of the choice of analytical lines for different matrix. In general, the best choice of analytical lines has to be determined by experiments. In addition, the fluctuation of the molten metal surface causes a poor stability of LIBS signal. It seems there has been no solution to this problem at present.

Sun *et al.* have developed a system as shown in Fig. 16 for online measurement of molten steel composition recently [37]. The system can semi-quantify the element of Cr, Mn, Ni and Si in molten steel. It should be pointed out that the homogeneity of the liquid steel is poor because various kinds of metal powder were added into the liquid steel and cannot be stirred by their furnace.

Fig. 16 The LIBS system for quasi online analysis of molten steel composition developed by Shenyang Automatic Institute of CAS.

Recently, Dong's group has developed an experimental system, which includes a light-guiding arm and an optical probe, to analyze the liquid slag (Fig. 17). The laser pulse with 600 mJ energy can be transported flexibly. The optical probe can transport laser pulses and collect plasma emission. Using this setup and a Si-Mo furnace some preliminary experiments for real-time analysis of a few molten slag samples have been carried out. A mathematical model developed by Lopez-Moreno [38] was used for calibration of the spectra. Table 5 is the measurement results and comparison with the values obtained by XRF.

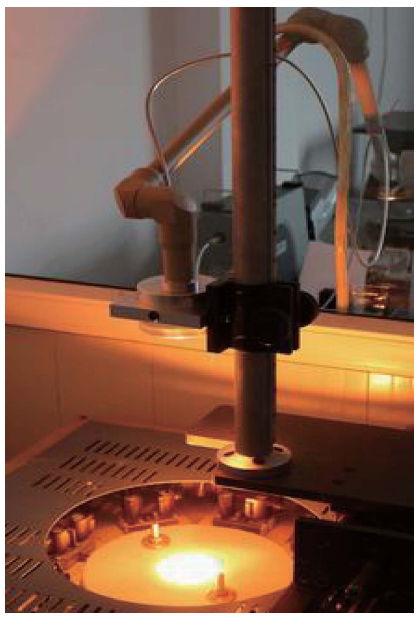

Fig. 17 Experimental set-up mounted on a furnace.

Three slag samples were analyzed. The measurement accuracy of Al_2O_3 and TiO_2 were satisfying.

Table 5 Online measurements of slag samples using LIBS technique.

		MnO	Al_2O_3	CaO	MgO	SiO_2	TiO_2
1#	XRF values	0.37	16.11	36.86	9.17	34.83	0.96
	Measurement values	0.38	15.72	35.94	10.46	40.90	0.99
	Relative error	2.7%	2.4%	2.5%	14.1%	17.4%	3.1%
2#	XRF values	0.34	16.13	38.04	9.80	34.10	0.91
	Measurement values	0.30	16.86	35.62	10.74	36.09	0.90
	Relative error	11.8%	4.5%	6.4%	9.6%	5.8%	1.1%
3#	XRF values	0.35	16.15	36.50	9.51	35.33	1.02
	Measurement values	0.38	15.81	39.73	7.26	27.02	0.99
	Relative error	8.6%	2.1%	8.8%	23.7%	23.4%	2.9%

6 Conclusions

This article has briefly reviewed the domestic progress particularly for application of metallurgical online analysis using LIBS technique. The advances obtained in this field have included the development of experimental setup, effective calibration methods and prototype LIBS system.

The emission lines of many trace elements in steel are hard to be excited. Double pulsed LIBS may solve this problem. In the future, double pulsed LIBS should be studied deeply. It is also needed to design LIBS probe for long-term operation under high temperature and dusty environment.

Online calibration method is a key factor for the success of quantitative analysis of molten metal. Internal calibration method has been demonstrated in laboratory, but in steel production field, there are no standard samples whose matrix is the same as those of the measuring samples. Quadratic nonlinear calibration has just been studied preliminarily. This method can utilize more spectra information and reduce the matrix effect. Calibration-free is a potential method that can overcome the matrix effect, but it faces many difficulties such as self-absorption, and lack of some parameters. ANN is another potential method to calibrate LIBS spectra. The structure of ANN and training model need to be further studied. The input of ANN is very important for the performance of the ANN.

Another key factor for online analysis of molten metal in steel work is how to overcome the obstacles of the harsh environment. The probe must be dustproof and fire resistant. Additionally, if the analytical target is molten steel, how to transport the laser beam through a thick layer of slag from top or from bottom to liquid steel is a problem.

In brief, effectual calibration method and appropriate probe are two crucial subjects for LIBS application in metallurgical online analysis and needed more attention for development at the present time.

Acknowledgements We acknowledge the financial support from the National Natural Science Foundation of China (Grant No. 11075184) and the Knowledge Innovation Program of the Chinese Academy of Sciences (Grant No. Y03RC21124).

References

1. J. B. Sirven, B. Bousquet, L. Canioni, L. Sarger, S. Tellier, M. Potin-Gautier, and I. Le-Hecho, Anal. Bioanal. Chem., 2006, 385(2): 256
2. F. H. Kortanbruck, R. Noll, P. Wintjens, H. Falk, and C. Becker, Spectrochim. Acta B, 2001, 56: 933
3. A. I. Whitehouse, J. Young, I. M. Botheroyd, S. Lawson, C. P. Evans, and J. Wright, Spectrochim. Acta B, 2001, 56(6): 2371
4. S. Duchene, R. Bruder, J.-B. Sirven, and V. Detalle, CMA4CH 2008, Mediterraneum Meeting, 2nd Ed., 2008
5. D. Anglos, V. Zafiropulos, K. Melessanaki, M. J. Gresalfi, and J. C. Miller, Appl. Spectrosc., 2002, 56(3): 423
6. S. Tzortzakis, D. Anglos, and D. Gray, Opt. Lett., 2006, 31(8): 1139
7. Haizhou Wang, Advancing Front of Metallurgical Analysis, Beijing: Beijing Science Press, 2004
8. J. Gruber, J. Heitz, H. Strasse, D. Bauerle, and N. Ramaseder, Spectrochim. Acta B, 2001, 56(6): 685
9. J. Gruber, J. Heitz, N. Arnold, D. Bäuerle, N. Ramaseder, W. Meyer, J. Hochörtler, and F. Koch, Appl. Spectrosc., 2004, 58(3): 457
10. L. Peter, V. Sturm, and R. Noll, Appl. Opt., 2003, 42(30): 6199
11. V. Sturm, H. U. Schmitz, T. Reuter, R. Fleige, and R. Noll, Spectrochim. Acta B, 2008, 63(10): 1167
12. N. J. Yao, J. W. Chen, Z. J. Yang, and H. Z. Wang, Spectroscopy and Spectral Analysis, 2007, 27(7): 1452
13. J. M. Fan, G. X. Yan, X. Y. Zhang, X. H. Ji, R. E. Zheng, and Z. F. Cui, Chin. J. Lasers, 2010, 37: 1957
14. Z. N. Wang, Y. Li, Q. Y. Zhang, Y. Lu, and R. E. Zheng, Spectroscopy and Spectral Analysis, 2011, 31(6): 1697
15. G. W. Xu, X. Y. Lu, X. W. Du, S. B. Wang, and Q. P. Wang, Analytical Instrumentation, 2010, 174: 7
16. D. H. Zhu, X. W. Ni, J. P. Chen, and H. C. Zhang, Spectroscopy and Spectral Analysis, 2011, 31(2): 319
17. J. Z. Chen, S. J. Yu, J. Sun, L. J. Zhang, and X. Li, High Power Laser and Particle Beams, 2011, 23: 205
18. C. L. Xie, J. D. Lu, Y. Li, and Z. X. Lin, J. Huazhong Univ. Sci. & Tech., 2008, 36: 114
19. Q. Wang, F. Z. Dong, Y. X. Liang, X. L. Chen, J. G. Wang, B. Wu, and Z. B. Ni, Acta Opt. Sin., 2011, 31: 1030002
20. L. X. Sun and H. B. Yu, Spectrochim. Acta B, 2009, 64(3): 278
21. M. C. Jiang, J. D. Lu, S. C. Yao, S. H. Pan, K. Chen, and M. R. Dong, Spectroscopy and Spectral Analysis, 2010, 30(10): 2797
22. Q. Wang, X. L. Chen, R. H. Yu, M. M. Xu, Y. Yang, B. Wu, Z. B. Ni, and F. Z. Dong, Spectroscopy and Spectral Analysis, 2011, 31(9): 2546
23. A. Ciucci, M. Corsi, V. Palleschi, S. Rastelli, A. Salvetti, and E. Tognoni, Appl. Spectrosc., 2002, 56: 960
24. X. L. Chen, F. Z. Dong, Q. Wang, R. H. Yu, Y. X. Liang, J. G. Wang, Y. Yang, Z. B. Ni, M. M. Xu, and B. Wu, Spectroscopy and Spectral Analysis, 2011, 31(12): 3289
25. D. Bulajic, M. Coris, G. Cristoforetti, S. Legnaioli, V. Palleschi, A. Salvetti, and E. Tognoni, Spectrochim. Acta B, 2002, 57(2): 339
26. L. X. Sun and H. B. Yu, Talanta, 2009, 79(2): 388
27. S. Laville, M. Sabsabi, and F. R. Doucet, Spectrochim. Acta B, 2007, 62(12): 1557
28. L. X. Sun, H. B. Yu, Y. Xin, and Z. B. Cong, Spectroscopy and Spectral Analysis, 2010, 30(12): 3186
29. L. X. Sun, H. B. Yu, Z. B. Cong, and Y. Xin, Acta Opt. Sin., 2010, 30: 2757
30. Y. X. Liang, X. L. Chen, Q. Wang, J. G. Wang, Y. Yang, Z. B. Ni, and F. Z. Dong, Journal of Atmospheric and Environmental Optics (accepted)
31. X. X. Lin, J. Q. Cao, Q. H. Yin, and X. Q. Liu, Ferro-Alloys, 2009, 204: 41
32. G. Hubmer, R. Kitzberger, and K. Mörwald, Anal. Bioanal. Chem., 2006, 385(2): 219
33. K. Chen, J. D. Lu, and J. Y. Li, Spectroscopy and Spectral Analysis, 2011, 31(3): 823
34. S. H. Pan, J. D. Lu, K. Chen, S. C. Yao, J. Y. Li, M. R. Dong, and J. Li, Appl. Laser, 2010, 30: 329
35. M. R. Dong, J. D. Lu, J. Li, K. Chen, S. H. Pan, S. C. Yao, and J. Y. Li, Acta Opt. Sin., 2011, 31: 0130002-1
36. L. X. Sun, H. B. Yu, Y. Xin, Z. B. Cong, and H. Y. Kong, Chin. J. Lasers, 2011, 38: 0915002
37. L. X. Sun, H. B. Yu, Z. B. Cong, and Y. Xin, Chin. J. Sci. Instrum., 2011, 32: 2602
38. C. Lopez-Moreno, S. Palanco, and J. J. Laserna, Spcetrochim. Acta B, 2005, 60(7–8): 1034
39. L. X. Sun and H. B. Yu, Spectroscopy and Spectral Analysis, 2009, 29: 3375
40. Y. Z. Lu, J. S. Wang, D. P. Qiao, J. J. Zheng, and Y. Tang, Metallurgical Analysis, 2010, 30: 10
41. D. X. Sun, M. G. Su, C. Z. Dong, X. L. Wang, D. C. Zhang, and X. W. Ma, Acta Phys. Sin., 2010, 59: 4571